TECHNICAL TRANSACTIONS | CZASOPISMO TECHNICZNE
CIVIL ENGINEERING | BUDOWNICTWO
1-B/2013

KRZYSZTOF GROMYSZ*

DISSIPATIVE FORCES IN JOINT SURFACE OF COMPOSITE REINFORCED CONCRETE FLOORS

SIŁY ROZPRASZAJĄCE ENERGIĘ W ZESPOLENIU ŻELBETOWYCH STROPÓW WARSTWOWYCH

Abstract

It is assumed that longitudinal shearing in joint surface (interface) of composite floors is balanced by: elastic forces, force of cohesion and kinetic friction. Moreover, internal friction occurs in the interface. Due to their nature, not all the above mentioned phenomena occur at the same time; however they are together responsible for deformation of interface. The paper discusses dissipative forces (non elastic). An interface model is built and test results of six floors are presented. All slabs are the same size – 3 m span and 0.6 m width and 0.18 m high. All slabs have the same longitudinal reinforcement. There are four types of join surface tested: smooth, very smooth, with eliminated adhesion and indented.

Keywords: Composite floor, concrete structures, dissipative forces

Streszczenie

Przyjęto, że siły podłużnego ścinania w płaszczyźnie zespolenia żelbetowych stropów warstwowych są równoważone przez: siły sprężyste, kohezję oraz tarcie kinetyczne. Ponadto w zespoleniu pojawia się tarcie wewnętrzne. Ze względu na swoją naturę nie wszystkie siły wywoływane są równocześnie, jednakże wspólnie odpowiadają za obserwowane odkształcenia w zespoleniu. W artykule zrelacjonowano badania sześciu płyt, które cechowały się takimi samymi wymiarami – rozpiętość 3 m, szerokość 0,6 m, wysokość 0,18 m i taką samą ilością zbrojenia przęsłowego. W płytach zastosowano cztery rodzaje powierzchni zespolenia: gładką, bardzo gładką, z usuniętą przyczepnością oraz z wrębami.

Słowa kluczowe: stropy zespolone, konstrukcje żelbetowe, siły rozpraszające energię

* Phd. Eng. Krzysztof Gromysz, Department of Building Structures, Silesian Technical University.

1. Introduction

Steel reinforced composite floors consist of two layers of concrete: the bottom one being a prefabricated slab and a top one which is cast in situ. The surface of the prefabricated element is usually rough or indented. Transverse reinforcement protrudes from the prefabricated slab (Fig. 1). The prefabricated slab serves as a form-work for cast in situ concrete.

Capacity of one-way steel reinforced concrete composite floor depends on several factors [1]: capacity of main reinforcement anchored in support, bending capacity but mainly the capacity of the shear stress in joint surface (interface) [2].

Longitudinal shear in the interface of two concretes in element of width b, according to [3] is equal to:

$$q_{Sj} = \frac{V}{z}, \tag{1}$$

where:

V – transverse shear force and z is the lever arm of the composite section.

The model of interface between concretes is the contact layer (Fig. 2). In this layer, shear stress causes elastic and plastic strains. Thus, the longitudinal shear in the interface q_{sj} in the assumed model is balanced by elastic force (conservative force) and non-elastic (non-conservative force). Occurrence of elastic force q_{el} is caused by non-dilatational elastic strain of the contact layer and elastic strain of transverse reinforcement. The value of restoring forces is the arithmetic product of displacement of top and bottom layers of concrete (w) and stiffness of the contact layer ($k_{q,w}$) [4]. The value of $k_{q,w}$ varies in the broad brackets from 1 GPa to 140 GPa and was the subject of the research presented in [5–6].

Occurrence of dissipative forces, which are the subject of research presented in the paper, depends on initial cohesion (q_{coh}) and kinetic friction ($q_{fr\text{-}int}$) that appears in the interferance between top layer and bottom layer. In the interferance, internal friction also occurs, which in the model discussed below does not transmit loading, but is responsible for maintaining plastic strain. Due to its nature, not all the above mentioned phenomena occur at the same time; however they are together responsible for contact layer strain. The analysis leads to the obvious conclusion that longitudinal shear in interface causes elastic and plastic strain. The two types of strain always occur at the same time and are caused by two corresponding forces: elastic force and dissipative force.

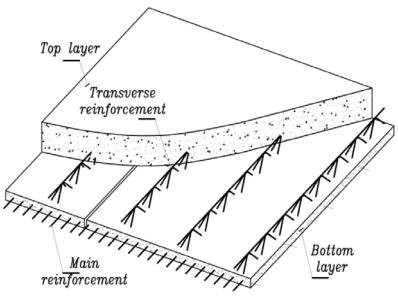

Fig. 1. Unidirectional reinforced concrete composite floor

The paper analyses work of dissipative forces occurring in the contact layer and compares it to energy accumulated in the layer. Analysis of dissipative forces occurring in the interface of composite floors wasn't done before. In the former author's paper just capacity of selected slabs and interface stiffness were investigated.

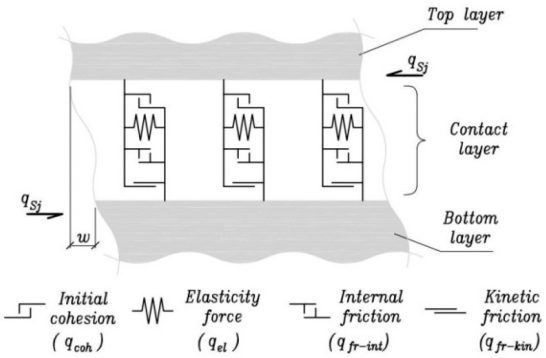

Fig. 2. Contact layer as a model of interface between top layer and bottom layer. Forces q_{coh}, q_{el}, $q_{fr\text{-}int}$, $q_{fr\text{-}kin}$ are balancing longitudinal shearing q_{sj}

2. Research of interface in composite floors

The research concerns six simply supported slabs, each of 3300 mm length, 590 mm width, 180 mm height and 3000 mm span. Five slabs: P1, P3, P4, P5, P6 were composite slabs, while one – P2 was a monolithic slab.

The bottom reinforcement of each slab consisted of six ribbed rebars of 20 mm diameter; their axis was 30 mm apart from the bottom surface of the slabs. In the case of five slabs P1, P2, P3, P4, P6 transverse reinforcement in form of two trusses made of plain bars of 6 mm diameter welded to main rebars were used (rebar number 2 shown in Fig. 3).

In the case of composite slabs, four types of joint surface were employed (Fig. 4):

– smooth – a free surface left without further treatment after vibration (P1, P6),
– very smooth – a surface cast against a plywood panel formwork (P3),
– with eliminated adhesion (P4),
– indented with indentations 5/5 mm every 50 mm, cast against a plywood panel formwork (P5).

In the case of composite slabs, the bottom layer was made first, the top layer was cast three weeks later. The very smooth surface and the indented surface were obtained by pouring the concrete into a positioned formwork in an upside-down orientation with the interface down. The bottom of the formwork was made of smooth plywood in the case of slabs P3 and P4, while in the case of slab P5, 5/5 mm battens were screwed every 50 mm to the plywood which gave indentations in the cast. The bottom layer of slabs P1 and P6 was prepared in traditional way – a free surface left without further treatment after vibration. On the top of the surface, cement wash appeared.

The width of the interface was equal to the slab's width or, as in the case of slab P6, was reduced to 200 mm. Description of slabs, their types and surface types is shown in Fig. 4.

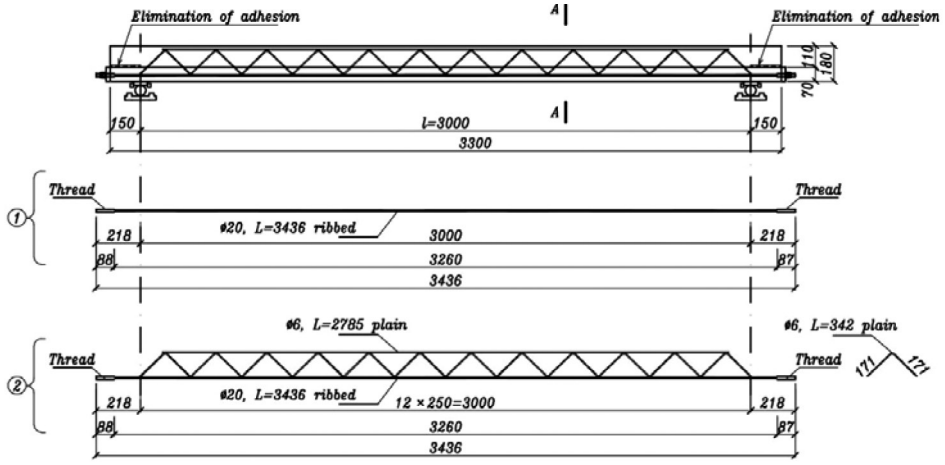

Fig. 3. Reinforcement of examined slabs. A-A sections of slabs are shown in Fig. 4

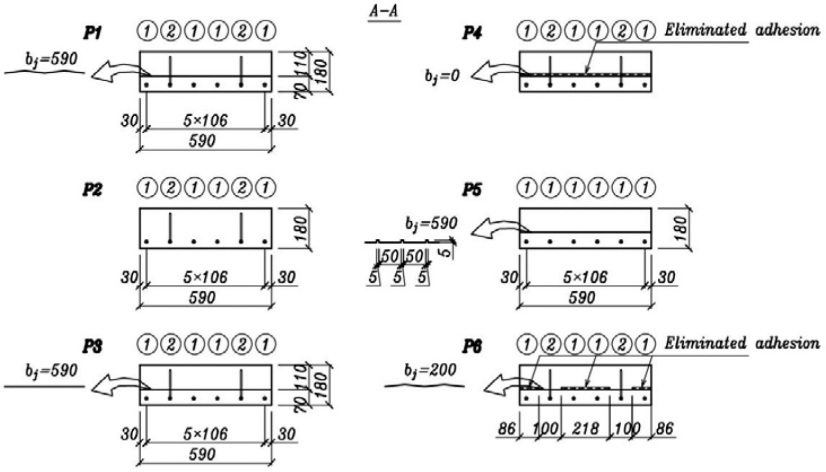

Fig. 4. Cross-sections of tested slabs, b_j – width of interface

Elimination of adhesion of two layers of concrete was ensured by two layers of oil covered foil. Moreover, in the case of all the slabs, adhesion was eliminated along the 150 mm parts of the joint surface beyond the axis of support. The following values were measured during the research:

– external loading force – Q (Fig. 5a),
– deflection in the centre of span – a (Fig. 5a),
– mutual displacement of bottom and top layers of concrete w_{7p}, w_{6p}, w_{5p}, w_{4p}, w_{3p}, w_{2p}, w_1, w_{2l}, w_{3l}, w_{4l}, w_{5l}, w_{6l}, w_{7l} (Fig. 5b, c),

Indices in denotation of layer displacement measurements include designation of symmetrically loaded slab side – "$_p$" denotes right side while "$_l$" denotes left side. Deflections and displacements were recorded with the use of a recording system, ensuring 0.001 mm

resolution. The testing system was ensuring applaying the Q force of resolution 0,01 kN. The level of resolution was the effect of analog-digital converter limitation and not inaccuracy of inductive sensors. The range of the measuring device was 20 mm.

All the slabs, apart from the two cases discussed below, were loaded in the centre of the span with concentrated force Q. Loading was increased from zero to a predetermined value, then the slab was unloaded. For each slab four predetermined levels of load force were used – these were denoted as Q_A, Q_B, Q_C and Q_D. Level Q_A corresponds to approximately 0.1 mm deflection in the midspan, level Q_B – 0.5 mm deflection, while level Q_C – 50% of tested load capacity of the slab. All slabs loaded with force Q_D (force Q_D is the tested load capacity) showed large deformation. The slabs were tested one month after the top layer of concrete was produced. The shrinkage of the top layer of concre effected the stress state of the contact layer but, due to short time of slab's loading, didn't effect the measurement results.

In the case of slabs P1 and P2, force was applied differently – force Q was divided into two forces (four-point bending), which is presented in Fig. 5a.

The above presented program of research is a part of broader research, including an evaluation of the hysteresis loop for the first three forms of free vibrations, modal studies and studies of free vibrations for different states of slabs. Results of this research will be presented in other publications.

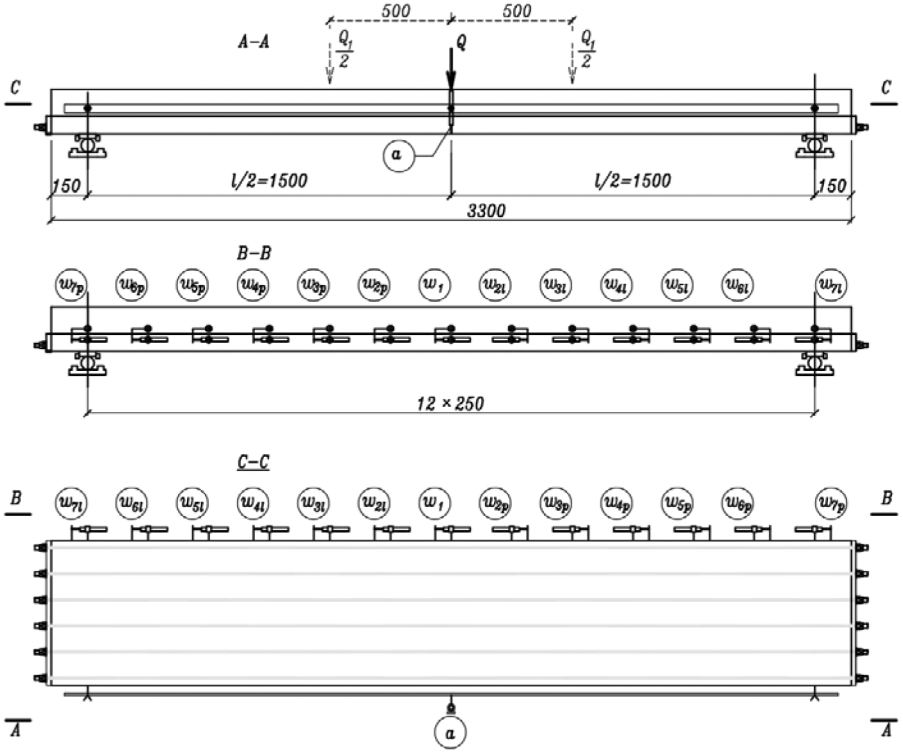

Fig. 5. Test setup for composite slab test

3. Test results

The research provided extensive investigational material. The paper is restricted to presenting those findings, which allow to describe non-conservative forces in joint surface. Fig. 6, 8 show measured values of displacement w_{ip} in function of loading, i.e. in correlation $w_{ip}(Q)$ for all composite slabs. Measurements for three loading-unloading cycles, corresponding to forces Q_A, Q_B and Q_C for slabs P4 and P6 are shown in Fig. 6 and Fig. 7. Results for slabs P1, P3 and P5 include values for cycles at loading force Q_C, only (Fig. 8). Resolution of the recording system did not allow for the recording of results corresponding to forces Q_A and Q_B.

Analysis of correlations $w_{ip}(Q)$ (Fig. 6, 8) allow for stating that all the slabs are characterised by a hysteresis loop, that is, the curve of loading does not overlap the curve of unloading and that permanent displacement in joint surface (w_r – Fig. 9) is observed after unloading. Moreover, it can be noticed, that in the case of all measurements the sensors closest to the place, where loading force was applied, that is w_{2p} and w_{3p}, recorded displacement practically from the beginning of loading. In the range of loading forces Q_A and Q_B in slabs P4 and P6 as well as in the range of loading force Q_C in slab P3, all the curves $w_{ip}(Q)$ in the part where loading force Q was increasing were almost straight. This observation was the basis for an assumption that the proportion of elastic and plastic strain is constant in the so called elastic phase of work in the interface.

Due to their shape, the hysteresis loops may be divided into two groups.

The first group includes curves presented in Fig. 6a, b, 7a, b, 8b, c in which the loading-unloading process proceed along approximately parallel straight curves. The hysteresis loop is a result of phase of unloading, when decrease in loading force Q does not cause a change in displacement of top and bottom (w) layers (also Fig. 9a).

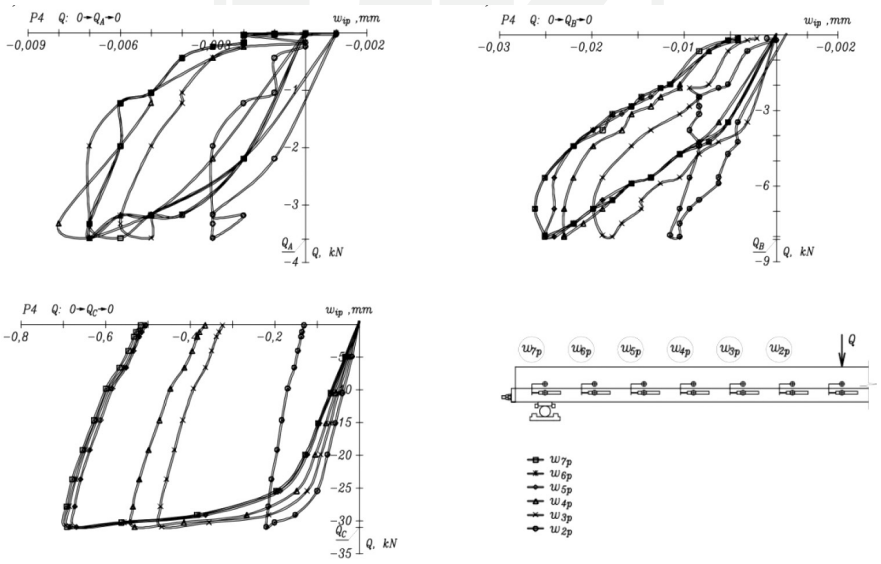

Fig. 6. Values of displacement in joint surface of slab P4 recorded in loading-unloading cycle corresponding to forces: a) Q_A, b) Q_B, c) Q_C

The second group includes curves presented in Fig. 6c, 7c, 8a. In this group, the process of loading consists of two segments: first one, in which curve(Q) corresponding to the loading process, is inclined at an acute angle in relation to the horizontal axis (also Fig. 9b – inclination $k_{w,fr\text{-}int}$), and the second one in which this curve is inclined at an obtuse angle to the horizontal axis (also Fig. 9b – inclination $k_{w,fr\text{-}kin}$). Curve segment $w(Q)$, corresponding to unloading, is parallel to the first curve segment of the loading process.

The type of joint surface does not determine whether curve $w_i(Q)$ belongs to the first or second group. For instance, for slab P6, curves shown in Fig. 7a, b belong to the first group while curves shown in Fig. 7c belong to the second group. The curves suggest that it is the value of displacement of two layers of concrete, corresponding to the maximum loading force Q, that decides whether it belongs to this or another group. If the maximum displacement is smaller than approximately 0.1 mm then the curve belongs to the group presented in Fig. 9a; if it is greater than approx. 0.1 mm, then the curve belongs to the group presented in Fig. 9b.

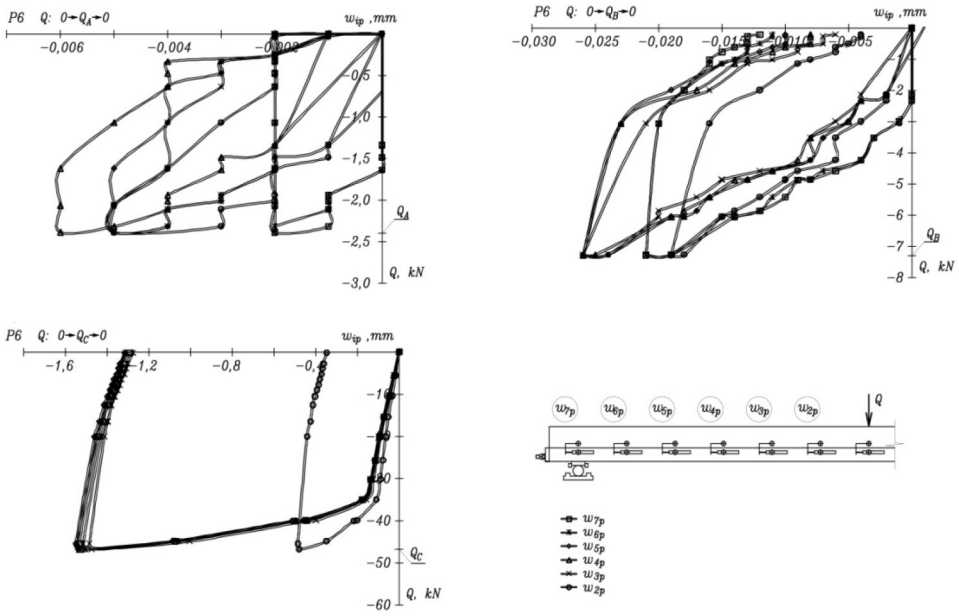

Fig 7. Diagrams of displacement in joint surface of slab P6 for loading-unloading cycles corresponding to forces: a) Q_A, b) Q_B, c) Q_C

In the case of slabs P1, P4 and P6, delamination occurred as an effect of loading. Slabs P2, P3 and P5 were no longer loaded, as significant deflection occurred after loading with Q_D (yield of main reinforcement).

Slabs were statically loaded with forces Q_A, Q_B, Q_C, generating corresponding deflections a_A, a_B, a_C whose values are presented in Table 1. After generating deflection, the slabs were statically unloaded. In the course of loading – unloading, cycle measurements were made of loading force, deflection and displacement according to Fig. 5. In the final stage of experiment, the slabs were loaded with load Q_D, which caused considerable deformation of slabs (slabs deflection was about 30 mm) that exceed the range of the measuring device.

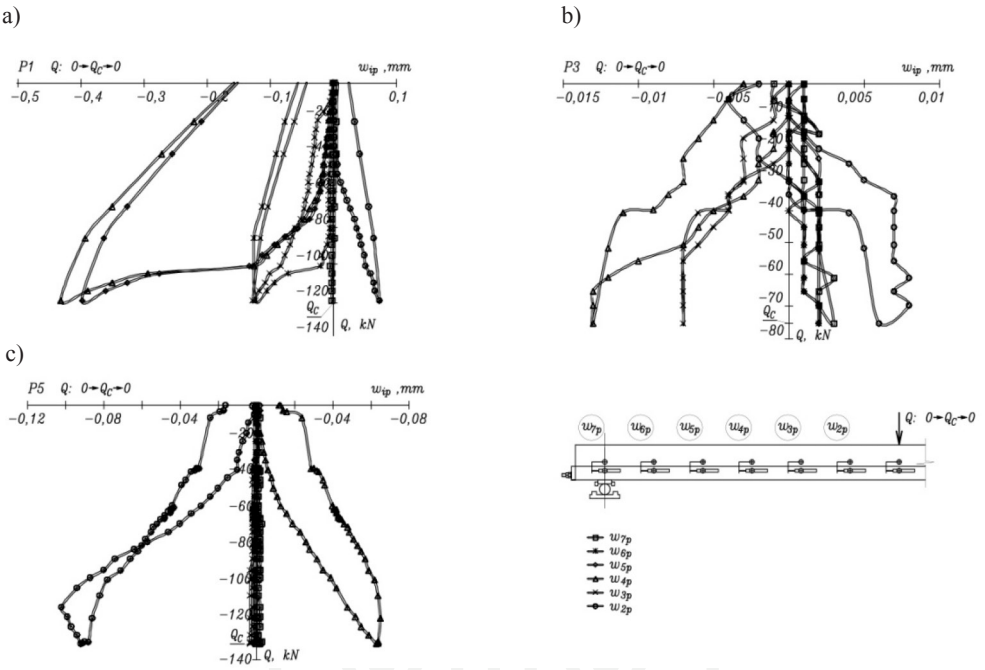

Fig. 8. Diagrams of displacement in joint surface recorded in loading-unloading cycle corresponding to Q_C force a) slab P1, b) slab P3, c) slab P5

Table 1

Maximum values of load forces (Q) and deflection in the centre of span (a) in cycles of loading

Element	Q_A [kN]	a_A [mm]	Q_B [kN]	a_B [mm]	Q_C [kN]	a_C [mm]	Q^*_D [kN]
P1	5.46	0.083	6.10	0.381	120.41	11.988	165
P2	3.56	0.107	11.30	0.493	139.97	13.434	265
P3	4.54	0.113	–	–	75.27	7.625	260
P4	3.58	0.122	8.03	0.536	31.01	9.618	45
P5	2.69	0.110	9.94	0.540	131.29	17.808	270
P6	2.39	0.126	7.30	0.542	46.95	17.411	74

* Deflection corresponding to load Q_D exceed the range of the measuring device equal to 20 mm

4. Test results interpretation

As shown above in the obtained curves of correlation, loading force (Q) displacement in joint surface (w) in the cycle of loading and unloading may be related to one of the two loops of hysteresis presented in Fig. 9. Appearance of this loop indicates that elastic strain is accompanied by plastic strain. The area of the loop is the measure of work performed by dissipative forces.

In agreement with the model (Fig. 2), it was assumed that in the case of the loop presented in Fig. 9a, the work was performed by internal friction force, while in the case of the loop presented in Fig. 9b, the work was performed by force of kinetic friction. Alteration of gradient of $Q(w)$ curve (Fig. 9b) in the course of loading indicates kinetic displacement of the bottom layer in relation to the top layer.

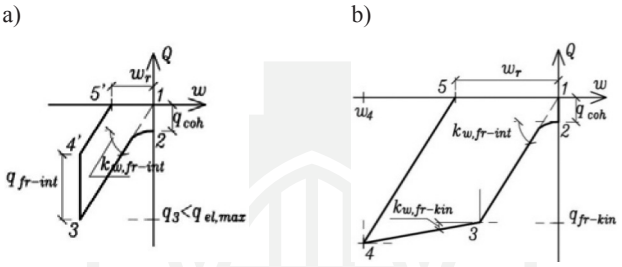

Fig. 9. Hysteresis loop of interface of composite floors: a) loop in the case when displacement $w < 0.1$ mm is caused by forces of internal friction ($q_{fr\text{-}int}$), b) loop in the case when displacement $w > 0.1$ mm is caused by forces of kinetic friction ($q_{fr\text{-}kin}$)

4.1. Energy dissipated by internal friction

When values (w_i, Q_i) are known, the area of the hysteresis loop denoted as ψ_w can be calculated from the formula:

$$\psi_w = \frac{1}{2}\sum_{i=1}^{n} Q_i \left(w_{i+1} - w_{i-1} \right) \tag{2}$$

This area is marked with horizontal lines on Fig. 10

The area in Fig. 10, which is marked with vertical lines, is the measure of potential energy accumulated in the joint surface at the moment when the slab was loaded with maximum loading. This area was denoted as $E_{p,w}$ and can be calculated from formula (2).

Table 2 shows individual loading – unloading cycles in which the value of displacement (w) did not exceed approximately 0.1 mm, determined measures ψ_w and $E_{p,w}$ as well as coefficient of energy dissipation defined as:

$$\chi = \frac{\psi_w}{E_{p,w}} \tag{3}$$

The results presented in this table show that in the case of slabs P1, P4 and P5, the value of the coefficient of energy dissipation χ_{stat} increases with distance from the point where loading force was applied. For instance, in slab *P*1 for cycle corresponding Q_C force, this value increases from 0.259 for measurement w_{2p} to 0.863 for measurement w_{7p}. In slab P4 for cycle corresponding to force Q_A, value χ_{stat} increases from 0.599 for measurement w_2 to 0.765 for measurement w_6, while in slab P6, the cycle corresponding to force Q_A increases from 0.315 (measurement w_2) to 0.923 (measurement w_7). The results also show that the increase of parameter χ is greater in the case of slabs P1 and P6, where concrete in contact layer also takes part in energy dissipation. In the slab P4, where the possibility of the generation of static friction stress on the surface of two layers of concrete was eliminated, energy is dissipated mainly by work performed by the surface of transverse reinforcement in the concrete canal.

Slabs P3 and P5, which show considerable value of elasticity coefficient and in which case no delamination occurred during destruction, are characterized by a lesser coefficient of energy dissipation. In these slabs, no increase of coefficient χ_{stat} value was observed with increase of distance from point of force application.

The obtained results allow for the assumption that along with decrease of amplitude of loading force *Q*, the value of coefficient χ increases at segments of slab which are further from point of force application. At sufficiently small amplitudes of exciting force and thus small deformation of slabs, segments of slabs close to support work as monolithic slabs, while in the area where force *Q* is applied, the slabs work as composite slab.

Table 2

Results of analysis of elastic and non-elastic forces in elastic phase of work of joint surface

P1, Q_C		w_{2p}	w_{3p}	w_{4p}	w_{5p}	w_{6p}	w_{7p}
$Q \in (0 \rightarrow Q_A \rightarrow 0$ kN) $a \in (0 \rightarrow a_A \rightarrow 0$ mm) $\chi_{mead} = 0{,}592$	$w_{i,max}$ [mm]	+0.073	–0.127	–0.430*	–0.362*	–0.127	–0.002
	ψ_w [N·m]	1.873	66.060	53.863	46.044	34.176	8.437
	$E_{p,w}$ [N·m]	7.245	101.01	98.73	83.39	50.48	9.777
	χ	0.259	0.654	0.546	0.552	0.677	0.863
P3, Q_C		w_{2p}	w_{3p}	w_{4p}	w_{5p}	w_{6p}	w_{7p}
$Q \in (0 \rightarrow Q_C \rightarrow 0$ kN) $a \in (0 \rightarrow a_C \rightarrow 0$ mm) $\chi_{mead} = 0{,}481$	$w_{i,max}$ [mm]	+0.008	+0.007	–0.013	+0.002	+0.002	+0.003
	ψ_w [N·m]	0.261	0.067	0.268	0.077	0.070	0.027
	$E_{p,w}$ [N·m]	–	0.257	0.573	0.098	0.105	0.124
	χ	–	0.259	0.467	0.790	0.671	0.216

P1, Q_C		w_{2p}	w_{3p}	w_{4p}	w_{5p}	w_{6p}	w_{7p}
P4, Q_A		w_{2p}	w_{3p}	w_{4p}	w_{5p}	w_{6p}	w_{7p}
$Q \in (0 \rightarrow Q_A \rightarrow 0$ kN) $a \in (0 \rightarrow a_A \rightarrow 0$ mm) $\chi_{mead} = 0{,}654$	$w_{i,\max}$ [mm]	–0.003	–0.006	–0.008	–0.007	–0.007	–0.007
	ψ_w [N·m]	0.0047	0.0092	0.0099	0.0118	0.0132	0.0124
	$E_{p,w}$ [N·m]	0.0078	0.0148	0.0186	0.0170	0.0173	0.0175
	χ	0.599	0.620	0.530	0.698	0.765	0.709
P4, Q_B		w_{2p}	w_{3p}	w_{4p}	w_{5p}	w_{6p}	$\mathbf{w}_{7p}$
$Q \in (0 \rightarrow Q_B \rightarrow 0$ kN) $a \in (0 \rightarrow Q_B \rightarrow 0$ mm) $\chi_{mead} = 0{,}527$	$w_{i,\max}$ [mm]	–0.011	–0.019	–0.022	–0.025	–0.025	–0.025
	ψ_w [N·m]	0.0241	0.0465	0.0524	0.064	0.0696	0.0699
	$E_{p,w}$ [N·m]	0.0529	0.0907	0.104	0.120	0.121	0.121
	χ	0.454	0.512	0.505	0.536	0.575	0.577
P5, Q_C		w_{2p}	w_{3p}	w_{4p}	w_{5p}	w_{6p}	w_{7p}
$Q \in (0 \rightarrow Q_c \rightarrow 0$ kN) $a \in (0 \rightarrow a_c \rightarrow 0$ mm) $\chi_{mead} = 0{,}494$	$w_{i,\max}$ [mm]	–0.102	–0.003	+0.065	–0.001	–0.001	+0.003
	$\psi_{\mathbf{w}}$ [N·m]	–	0.131	2.849	–	–	0.050
	$E_{p,w}$ [N·m]	–	0.253	5.277	–	–	0.118
	χ	–	0.517	0.539	–	–	0.426
P6, Q_A		w_{2p}	w_{3p}	w_{4p}	w_{5p}	w_{6p}	w_{7p}
$Q \in (0 \rightarrow Q_A \rightarrow 0$ kN) $a \in (0 \rightarrow a_A \rightarrow 0$ mm) $\chi_{mead} = 0{,}754$	$w_{i,\max}$ [mm]	–0.005	–0.005	–0.006	–0.005	–0.002	–0.002
	ψ_w [N·m]	0.0048	0.00580	0.00565	0.00520	0.00402	0.00413
	$E_{p,w}$ [N·m]	0.0090	0.0090	0.0085	0.0076	0.0040	0.004
	χ	0.531	0.645	0.667	0.686	0.999	0.994
P6, Q_B		w_{2p}	w_{3p}	w_{4p}	w_{5p}	w_{6p}	w_{7p}

P1, Q_C		w_{2p}	w_{3p}	w_{4p}	w_{5p}	w_{6p}	w_{7p}
$Q \in (0 \rightarrow Q_B \rightarrow 0$ kN) $a \in (0 \rightarrow a_B \rightarrow 0$ mm) $\chi_{mead} = 0{,}702$	$w_{i,\max}$ [mm]	–0.019	–0.026	–0.026	–0.026	–0.021	–0.021
	ψ_w [N·m]	0.0531	0.0672	0.0800	0.0862	0.0920	0.0954
	$E_{p,w}$ [N·m]	0.0880	0.117	0.121	0.124	0.111	0.113
	χ	0.604	0.577	0.660	0.698	0.827	0.847

* displacement in the range of 0.1 mm were exceeded

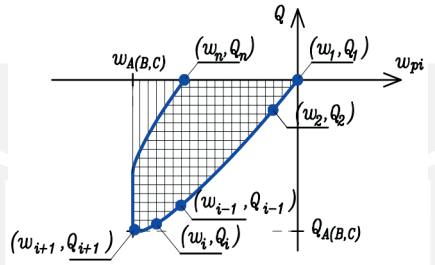

Fig. 10. Elastic potential energy $E_{p,w}$ in joint surface (area marked with vertical lines) and energy dissipated ψ_w at segment of joint surface (area marked with horizontal lines – the area of hysteresis loop)

4.2. Energy dissipated by kinetic friction

When the possibility of load transfer by elastic forces is exhausted, which is interpreted in the model as a loss of continuity of strain (w > 0.1 mm), forces of kinetic friction $\tau_{fr\text{-}kin}$ are generated in the joint surface. The model assumes that these forces are distributed uniformly along the joint surface and that they do not depend on loading. Increase of loading force Q effects in considerable increase of displacement between top and bottom layers (w).

In the course of discussed research kinematic friction, stress was generated in the joint surface of two slabs. In slab P4, it was generated under loading Q_{kin} = 25.05 kN while in slab P6, it ws generated under loading Q_{kin} = 35.20 kN. Values $q_{fr,kin}$ determined on equation (1), are equal correspondingly 98.24 kN/m and 138.04 kN/m.

It was also observed that relationship $Q(w_i)$ is not a straight line. It means that stiffness of the contact layer is a non-linear parameter. Similar was observed in [1, 7, 8–9].

Table 3

Values of kinetic friction stress in joint surface in non-elastic phase of work of joint surface

P4, Q_C	w_{2p}	w_{3p}	w_{4p}	w_{5p}	w_{6p}	w_{7p}
$w_{i,\max}$ [mm]	–0.220	–0.467	–0.532	–0.676	–0.684	–0.91
$w_{i,kin}$ [mm]	–0.075	–0.091	–0.104	–0.123	–0.128	–0.128
ψ_w [N·m]	3.611	10.075	11.301	14.838	14.947	15.166
P6 Q_C	w_{2p}	w_{3p}	w_{4p}	w_{5p}	w_{6p}	w_{7p}
$w_{i,\max}$ [mm]	–0.479	–1.483	–1.545	–1.545	–1.545	–1.533
$w_{i,kin}$ [mm]	–0.089	–0.123	–0.134	–0.136	–0.131	–0.136
ψ_w [N·m]	15.479	56.202	57.192	57.295	56.043	56.677

5. Conclusions

Performed experiments vindicate the model's assumption that shear in the interface of two concretes is balanced by elasticity forces and two kinds of non-elastic forces: initial cohesion and kinetic friction.

The outcome of the research indicates that in the interface between the top and bottom layers, internal friction appears. Internal friction appears when displacement between the top and bottom concrete layers is smaller than approximately 0.1 mm. This friction is responsible for generating the loop of hysteresis in the loading – unloading process, it means it is responsible for energy dissipation in the interface. The coefficient of the energy dissipation in the interface varies from 0.259 to 0.92. The value of the coefficient depends on the load value and the distance of considered cross-section from the place of applied concentrated load.

Kinetic friction appears in cases where mutual displacement of the bottom and top layers of concrete is larger than 0.1 mm. This friction takes part in balancing longitudinal shearing in the interface only when the stiffness of the contact layer is small. The value of kinetic friction varies in tested slabs of 0.59 m width, from 98.24 kN/m to 138.04 kN/m.

This paper was sponsored by program POIG.01.01.02-10-106/09-00.

References

[1] Halicka A., *A study of the stress – strain state in the interface and support zones of composite structures with shrinking and expansive concretes*, Wydawnictwo Politechniki Lubelskiej, Lublin 2007.

[2] Gromysz K., *Combined floors. Normative calculations guidecurves and capacity of actual structures*, 5-th international conference AMCM Analytical Models and New Concepts in Concrete and Masonry Structures, Gliwice-Ustroń June 12–14, 2005.

[3] Eurocode 2: Design of Concrete Structures – Part 1–1: General rules and rules for buildings. EN 1992-1-1:2004. European Committee for Standardization, Brussels, 2004.
[4] Gromysz K., *Longitudinal Shearing Balancing in Joint Surface of Composite Concrete Slabs.* Inżynieria i Budownictwo, 2010.
[5] Gromysz K., *Testing stiffness of contact layer in composite concrete slabs*, 56 Konferencja Naukowa Komitetu Inżynierii Lądowej i Wodnej PAN oraz Komitetu Nauki PZITB, Kielce–Krynica 19–24 września 2010.
[6] Gromysz K., *Calculation of deflection of delaminated reinforces concrete composite floor based on assumed frictional – elastic model of joint surface*, AMCM' 2008 6th International Conference, June 9–11, Łódź.
[7] Diazmati B., Pincheira J.A., *Shear Stiffness and Strength of Horizontal Construction Joints*. ACI Structural Journal, Vol. 101, No. 4, July–August 2004.
[8] Gohnert M., *Proposed theory to determine the horizontal shear between composite precast and in situ concrete*. Cement and Concrete Composites, No. 22, 2000.
[9] Momayez A., Ramezanianpour A.A., Rajaie H., Ehsani M.R., *Bi-Surface test for Evaluation Bond between Existing and New Concrete*, ACI Materials Journal, Vol. 101, No. 2, March–April 2004.